

Supporting Information

Automated Electrical Quantification of Vitamin B1 in a Bodily Fluid using an Engineered Nanopore Sensor

Florian Leonardus Rudolfus Lucas⁺, Tjemme Rinze Cornelis Piso⁺, Nieck Jordy van der Heide, Nicole Stéphanie Galenkamp, Jos Hermans, Carsten Wloka, and Giovanni Maglia**

anie_202107807_sm_miscellaneous_information.pdf

Table of Contents

MATERIALS	3
METHODS	3-6
COMPUTATIONAL PROCEDURES	6-7
THIAMINE DETERMINATION USING HPLC	7
REFERENCES	7
DETERMINATION OF LIGAND BOUND FRACTION USING EMPIRICAL BAYESIAN INFERENCE	8-10
Figure S1. Continuous trace of WT-TbpA in presence of thiamine	11
Figure S2. Representative signal of WT-TbpA with thiamine added to the <i>cis</i> chamber.....	12
Figure S3. Representative signal and binding curve of Y27A-TbpA with thiamine added to <i>trans</i>	13
Figure S4. Continuous trace of Y27-TbpA in presence of thiamine.....	14
Figure S5. Representative signal of Y27A-TbpA with thiamine added to the <i>cis</i> chamber.....	15
Figure S6. Representative signal snippets of Y27A-TbpA with thiamine added to the <i>trans</i> chamber....	16
Figure S7. Apparent on- and off-rates of thiamine binding to Y27A-Thiamine binding protein.....	17
Figure S8. FPLC result of thiamine and its phosphorylated derivatives.....	18
Figure S9. LC/ESI-MS result of thiamine and its phosphorylated derivatives.....	19

MATERIALS.

Chemicals.

Tris-(hydroxymethyl)-aminomethane hydrochloride (Tris.HCl), sodium chloride, and 2-amino-2-(hydroxymethyl)-1,3-propanediol (Tris.base), β -dodecylmaltoside (DDM), lysozyme, 2xYT-broth, LB-medium, TB-medium, ampicillin, agar-agar, agarose (broad-range), glucose, sucrose, glycerol, and imidazole were retrieved from Carl-Roth. DNase1, Phire II Hot Start Polymerase, Dpn1, isopropyl β -D-1-thiogalactopyranoside (IPTG) were retrieved from Fisher Scientific. Pentane and ethanol were acquired from Boomlab. 1,2-diphytanoyl-*sn*-glycero-3-phosphocholine (DPhPC), ethylenediaminetetraacetic acid (EDTA), magnesium chloride ($MgCl_2$), N-hexadecane, thiamine hydrochloride (ThOH), thiamine-(4-methyl- ^{13}C -thiazol-5-yl- $^{13}C_3$), thiamine monophosphate chloride dehydrate (ThMP) and thiamine pyrophosphate (ThDP) were received from Merck. Primers and synthetic genes were retrieved from Integrated DNA Technologies (IDT). Ni-NTA agarose beads were obtained from Qiagen. *E. cloni* 10G and *E. coli* BL21 (DE3) cells were originally retrieved from Lucigen. Polyacrylamide gels (PAGE) and Blue native polyacrylamide gel electrophoresis (BN-PAGE) was obtained from Bio-Rad. All solutions were prepared in ultrapure water (Milli-Q[®]), unless stated otherwise.

METHODS.

Purification of ClyA-AS. ClyA-AS was purified as described previously.^[1] In brief: ClyA-AS was transformed into *E. coli* BL21 (DE3) using a pT7-SC1 plasmid with an ClyA-AS insert.^[1,2] Transformants were grown overnight at 37 °C on a LB-agar plate supplemented with 100 mg/L ampicillin and 1% glucose. The (whole) LB-agar plate was used to inoculate 200 mL 2xYT medium supplemented with 100 mg/L ampicillin, which was grown at 37 °C under constant shaking (180 rpm) to $OD_{600}=0.6$, after which 0.5 mM IPTG was added and left to grow overnight at 25 °C under constant shaking (180 rpm). The cell culture was harvested using centrifugation for 20 min at 4 °C and 6000 rpm. The cell pellets were frozen for 1 hour at -80°C and

solubilized in 20 mL lysis buffer (150 mM NaCl, 15 mM Tris.HCl, pH 7.5, 1 mM MgCl₂, 0.2 unit/mL DNase1, 10 mM imidazole, 10 µg/mL lysozyme). Lysis was performed by incubation for 20 minutes at room temperature and sonication (Branson). Pellet cell debris was removed by centrifugation (6500 rpm, 30 min, 4 °C). Monomers were purified using Ni-NTA affinity purification. ClyA-AS monomers were incubated for 30 min at 37 °C in 150 mM NaCl, 15 mM Tris.HCl (pH 7.5) and 0.02% DDM. The oligomeric forms and monomers were separated using 4-20% polyacrylamide gels and blue native polyacrylamide gel electrophoresis. The band corresponding to Type 1 ClyA-AS was cut out and stored in-band until used. Oligomer containing bands were extracted using 150 mM NaCl, 15 mM Tris.HCl (pH 7.5) supplemented with 0.2 % DDM and 10 mM EDTA.

Cloning of TbpA. A synthetic gene containing His₆-tagged TbpA was inserted into a pT7-SC1 vector using standard TOPO cloning.^[3]

Expression of TbpA. TbpA (wild-type and mutant) was expressed by *E. coli* BL21 (DE3) containing a pT7-SC1 plasmid with a His₆-tagged TbpA insert. The *E. coli* BL21 (DE3) cells were grown overnight on a LB-agar plate supplemented with 100 mg/L ampicillin and 1% glucose at 37 °C. A single colony was inoculated into 10 mL LB-medium supplemented with 100 mg/mL ampicillin for 4 hours at 37 °C while shaking (180 rpm). The 10 mL starter was used to inoculate 1 L TB-medium supplemented with 100 mg/L ampicillin. The TB-medium was left to grow to OD₆₀₀~0.6 at 37 °C while shaking (180 rpm), after which the temperature was lowered to 20 °C until OD₆₀₀~1.2. Upon reaching OD₆₀₀~1.2, the culture was induced using 0.5 mM IPTG and left to grow overnight.

Purification of TbpA. Overnight (induced) cell pellets were collected using centrifugation at 4000 rpm for 30 minutes at 4 °C. The cell pellets (1 L of growth) were resuspended in 200 mL ice-cold sucrose buffer,

containing 20% Sucrose (w/v), 50 mM Tris.HCl pH 7.5 and 1 mM EDTA, and incubated for 30 minutes under rotation at room temperature. Washed pellets were collected using centrifugation at 7500 rpm for 10 minutes at 4 °C. The pellets were resuspended in 200 mL ice-cold 5 mM MgCl₂ and incubated for 1 hour at room temperature while under constant rotation. The solution was centrifuged at 7500 rpm for 30 minutes at 4 °C and the supernatant was loaded onto a Ni-NTA affinity column. The Ni-NTA affinity column was extensively washed with 100 mL of 50 mM Tris.HCl pH 7.5, 1M NaCl, 20 mM imidazole and 1% glycerol followed by a wash with 200 mL of 50 mM Tris.HCl pH 7.5, 150 mM NaCl, 20 mM imidazole and 1% glycerol. TbpA was eluted using 5 steps of 5 mL elution buffer containing 50 mM Tris.HCl pH 7.5, 150 mM NaCl, 300 mM imidazole and 1% glycerol. The purest fractions were combined and concentrated using 30 kDa cut-off Amicon Ultra Centrifugal Filters.

Construction of Y27A-TbpA. The Y27A point mutations was introduced to TbpA using site-directed mutagenesis.^[4] The His₆-tagged TbpA plasmid was mutated using two complementary primers, forward (CCCGTGTGACTGTGTACA CGGCAGACAGT) and reverse (CCAGTCTTGCCGCAA^{AA}ACTG TCTGCCGTGTA) using Phire II Hot Start Polymerase with a final volume of 50 µL. Thermal cycle: 30 seconds 98 °C followed by 30 cycles of denaturation 98 °C for 5 seconds, annealing 59 °C for 30 seconds and elongation 72 °C for 180 seconds followed by an elongation step of 300 seconds at 72 °C. The plasmid template was removed by incubating the PCR product with Dpn1 (1 FDU) for 2 hours at 37 °C. The product was incorporated into electro competent *E. coli*® 10G cells. Transformants were grown overnight at 37 °C on LB-agar plates supplemented with 100 mg/L ampicillin and 1% glucose. Single colonies were grown in 5 mL LB-medium supplemented with 100 mg/L ampicillin and DNA was extracted using QIAprep® Spin Miniprep. The incorporation of the mutation was confirmed by MacroGen EZ-seq standard direct sequencing.

Protein sequence of Y27A-TbpA.

MGSSHHHHHSSGLVPRGSHMKPVLTVYTADSFAADWGPVVKKAFAEADCNCELKLVLEDGVSLNRLRMEGKNS
KADVVLGLDNNLLDAASKTGLFAKSGVAADAVNVPGGWNNDTFVFPDYGYFAFVYDKNKLNPPQSLKELVESDQNW
RVYIQDPRTSTPGLGLLLWMQKVYGDAPQAWQKLAKKTVTVTKGWSEAYGLFLKGESDLVLSYTTSPAYHILEEKDNY
AAANFSEGHYLQVEVAARTAASKQPELAQKFLQFMVSPAFQNAIPTGNWMMYPVANVTLPAGFEKLTKPATLEFTPAEV
AAQRQAWISEWQRAVSR

DNA sequence of Y27A-TbpA.

ATGGGTTCTCCCACCATCACCATCATCATTCGAGTGGACTGGTCCCCCGCGTTTCGCACATGAAGCCCGTGTGACT
GTGTACACGTATGACAGTTTTGCGGCAGACTGGGGTCCCGGGCCCGTAGTGAAAAAGGCTTTTGAAGCGGATTGTA
ATTGTGAGTTGAAGTTGGTAGCCTTAGAAGATGGGGTATCACTTCTGAACCGCCTTCGTATGGAAGGTAAGAACTCC
AAGCCGACGTTGTGTTGGGCTTGGATAATAATTTGCTTGATGCCGCGAGTAAGACTGGCCTGTTTCGCTAAGTCTGG
AGTGCCGCTGATGCAGTGAACGTACCCGGTGGATGGAACAACGACACCTTTGTGCCATTGATTACGGTTACTTCG
CCTTCGTGTACGACAAGAATAAGTTAAAGAATCCCCCAATCACTGAAAGAACTTGTTGAGTCTGATCAGAACTGGC
GTGTGATCTATCAGGACCCGCGCACCTCGACCCCGGGCTTGGGACTGTTGCTTTGGATGCAGAAAGTGACGGTGAC
GATGCCCCGCAAGCATGGCAGAACTGGCTAAGAAAACCGTAACTGTCACAAAAGGGTGGAGCGAAGCATAACGGC
TTATTCCTGAAGGGTGAGAGCGACCTTGCCTTTTCGTATACTACGTCTCCAGCATACCATATTTGGAGGAAAAGAAA
GACAACTATGCAGCGGCTAACTTCTCGGAAGGTCATTACCTTCAAGTGGAAGTTGCTGCCCGCACAGCCGCGTCGAA
GCAACCGGAGTTGGCTCAAAAATTTCTGCAGTTCATGGTTAGCCCCGCTTTTCAGAACGCCATCCCCACTGGCAACT
GGATGTACCCGGTGGCAAACGTTACCCTGCCTGCTGGATTTGAGAAATTGACAAAAGCCAGCTACAACATTAGAATTT
ACCCAGCGGAGGTAGCAGCACAGCGTCAGGCCTGGATCTCAGAATGGCAGCGTGCAGTGTCTCGTTGA

Black lipid membrane electrophysiological recordings. A two compartment recording chamber consisting of two polyoxymethylene cuvettes (600 μ L, described in an earlier study)^[5] separated using a 25 μ m thick

Teflon membrane, with an aperture diameter of approximately 100 μm , was used. 5 μL of 2.5% hexadecane in pentane was applied to both sides of the aperture and left to dry for 1 minute. 500 μL of buffer (150 mM NaCl, 15 mM Tris.HCl, pH 7.5) was added to both compartments topped with 20 μL of 12.5 mg/mL DPhPC in pentane, the pentane was left to evaporate for 2 minutes. A silver/silver chloride electrode was inserted into the *cis* and the *trans* compartment and connected to the ground and working electrode of the Axon 200b amplifier, respectively. Lipid bilayers were created at the aperture using the Langmuir-Blodgett method described by Maglia *et al.* ^[5] The orientation of ClyA nanopores was determined by the asymmetry of the current-voltage relationship. 15 nM TbpA was added to the *cis* compartment and well mixed (unless stated otherwise). Thiamine was added to either the *cis* or *trans* compartment.

Data acquisition. Ionic current data was acquired using two instruments. **Setup A** (Figure 2 and 3): an Axopatch 200B amplifier combined with a Digidata 1550B A/D converted, both obtained from Axon instruments, was used. Similar to preceding work,^[5,6] recordings were made using the Clampex 10 software, recording at a sampling frequency of 10 kHz using an analogue Bessel filter of 2 kHz. The final bandwidth was reduced to 10 Hz for analysis using a digital Gaussian filter. **Setup B** (in Figure 4): an eOne XV (elements SRL) operating on hereby presented software was used at a sampling frequency of 20 kHz, digitally filtered down to 10 kHz. The final bandwidth was reduced to 10 Hz for analysis using a digital Gaussian filter.

COMPUTATIONAL PROCEDURES.

Data analysis. Electrophysiology traces were analyzed using Jupyter Notebook (version 5.5.0), implemented in the Anaconda (version 5.2.0) environment supported by Python 3.6.5 (64-bit). Module packages not included in Anaconda (version 5.2.0) were installed from PyPi using pip (version 10.0.1)

unless stated otherwise. Neo (version 0.7.1) was used to load Axon Binary Format traces into NumPy arrays (NumPy version 1.14.3). Events were detected, and the bound fraction was estimated using the algorithm as described in this contribution (Recursive Event Detection). Corrected Hill functions were fitted using curve fit optimizer as implemented in SciPy (version 1.1.0).

THIAMINE DETERMINATION USING HPLC. Urine samples were stored at -25 °C, thawed on the day of analysis. Thawed samples were pre-treated by addition of formic acid to a final concentration of 0.1% (pH 3). Prior to analysis, the standard mixtures (sample + standard) were vortexed and centrifuged for 10 minutes at 20 000 rpm. The supernatant was used for analysis. The quantification of thiamine was performed using a Prominence LC-20AD (Shimadzu Europa GmbH, Duisburg, Germany) equipped with an analytical Discovery C18 column (2.1 x 100 mm, 5 µm, Supelco, Bellefonte, USA), connected to a TSQ Quantum Ultra™ Mass Spectrometer (Thermo Electron, San Jose, USA). The mobile phase consisted of 4.8 mM ammonium bicarbonate, pH 7.9 (solvent A) and acetonitrile (solvent B). An isocratic program of 50% solvent B for 10 minutes at a flow rate of 0.25 mL/minute and a sample injection volume of 2 µL was used. The thiamine concentration was determined using a thiamine-(4-methyl-¹³C-thiazol-5-yl-¹³C₃)-labelled internal standard at a concentration of 1 µM, and a calibration curve of ThOH between 0.05 µM to 10 µM, containing 0.1% formic acid in all samples.

REFERENCES.

- [1] N. S. Galenkamp, V. Van Meervelt, N. L. Mutter, N. J. van der Heide, C. Wloka, G. Maglia, **2021**, pp. 11–18.
- [2] N. S. Galenkamp, M. Soskine, J. Hermans, C. Wloka, G. Maglia, *Nat. Commun.* **2018**, *9*, 4085.
- [3] S. Shuman, *J. Biol. Chem.* **1994**, *269*, 32678–32684.
- [4] J. Braman, C. Papworth, A. Greener, in *Vitr. Mutagen. Protoc.*, Humana Press, New Jersey, **n.d.**, pp. 31–44.
- [5] G. Maglia, A. J. Heron, D. Stoddart, D. Japrun, H. Bayley, in *Methods Enzym.*, **2010**, pp. 591–623.
- [6] C. Wloka, N. L. Mutter, M. Soskine, G. Maglia, *Angew Chem Int Ed Engl* **2016**, *55*, 12494–12498.

1. Determination of ligand bound fraction using empirical Bayesian inference

We determine the bound fraction of the *ligand-bound* level using empirical Bayesian inference²⁹, which allows the estimation of the bound fraction on sparse data.

$$\theta = a + b * \left(\frac{[L]^n}{K_d + [L]^n} \right), \quad [\text{Hill} - \text{Langmuir equation}] \quad (1)$$

Where θ is the bound fraction observed given the ligand concentration $[L]$. The constant a represents the offset to correct for intrinsic closing and b represents the normalization factor. K_d is the apparent dissociation constant and n represents the Hill coefficient. With the binding affinity is either positively ($n > 1$), negatively ($n < 1$) or not ($n = 1$) influenced by analyte binding.

We rewrite the Hill-Langmuir equation in terms of the normalized bound fraction, which results in **equation 2**, and insert the equation to calculate the dissociation constant from the on and off rate resulting in **equation 3**.

$$\tilde{\theta} = \frac{\theta - a}{b} = \left(\frac{[L]^n}{K_d + [L]^n} \right) \quad (2)$$

Replace K_d using the dissociation constant equation such that $K_d = \frac{k_{off}}{k_{on}}$,

$$\tilde{\theta} = \frac{k_{on}}{k_{on}} * \frac{[L]^n}{\left(\frac{k_{off}}{k_{on}} + [L]^n \right)} = \frac{[L]^n * k_{on}}{k_{off} + [L]^n * k_{on}} \quad (3)$$

We rewrite equation 3 in terms of time spend in the *apo* (**equation 4**) and ligand bound (**equation 5**) state.

The resulting (**equation 6**) can be expressed as the probability of finding the liganded state $\{P(\text{ligand})\}$ relative to the total probability of finding the liganded and *apo* state $\{P(\text{apo})\}$. We determine the

probability of finding the liganded state (**equation 7**) and probability of finding the *apo* state (**equation 8**) based on the data (\mathcal{D}) using Bayes theorem.

$$event_{time}(apo) = \frac{1}{[L]^n * k_{on}} \quad (4)$$

$$event_{time}(ligand) = \frac{1}{k_{off}} \quad (5)$$

$$\tilde{\theta} = \frac{event_{time}(apo)^{-1}}{event_{time}(ligand)^{-1} + event_{time}(apo)^{-1}} = \frac{event_{time}(ligand)}{event_{time}(ligand) + event_{time}(apo)} = \frac{P(ligand|\mathcal{D})}{P(ligand|\mathcal{D}) + P(apo|\mathcal{D})} \quad (6)$$

$$P(ligand|\mathcal{D}) = \frac{P(\mathcal{D}|ligand) * P(ligand)}{P(\mathcal{D})} \quad (7)$$

$$P(apo|\mathcal{D}) = \frac{P(\mathcal{D}|apo) * P(apo)}{P(\mathcal{D})} \quad (8)$$

Where $P(ligand|\mathcal{D})$ is the probability of the ligand state given the data, $P(\mathcal{D}|ligand)$ is the probability of the data given the ligand state, $P(ligand)$ is the probability of the ligand state and $P(\mathcal{D})$ is the probability of the data. Where $P(apo|\mathcal{D})$ is the probability of the *apo* state given the data, $P(\mathcal{D}|apo)$ is the probability of the data given the *apo* state, $P(apo)$ is the probability of the *apo* state and $P(\mathcal{D})$ is the probability of the data.

Prior to analysis of an unknown sample, we use the control (for *apo*) and ligand-saturated (for *ligand-bound*) traces to determine the prior probabilities for the *apo* $\{P(apo)\}$ and ligand-bound state $\{P(ligand)\}$. During real-time analysis, we determine the empirical likelihood $P(\mathcal{D}|apo, ligand)$ from the full point histogram of protein blockades that contain the I_{apo} . We take peak drifting into account by allowing the centers of the prior probabilities to shift an equal amount. The bound fraction is calculated as the fraction between the *apo* and ligand states (**equation 9.**)

$$\tilde{\theta} = \frac{P(ligand|\mathcal{D})}{P(ligand|\mathcal{D}) + P(apo|\mathcal{D})} = \frac{P(\mathcal{D}|ligand) * P(ligand)}{P(\mathcal{D}|ligand) * P(ligand) + P(\mathcal{D}|apo) * P(apo)} \quad (9)$$

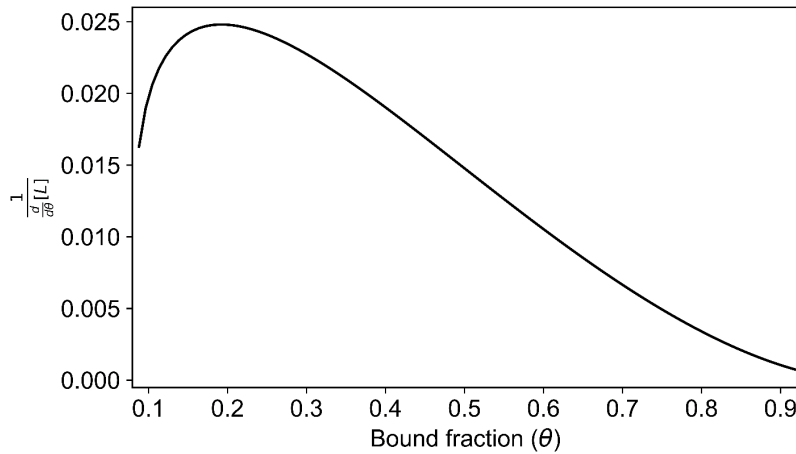
We estimate the bound fraction based on snippets of 1 second blocked time (protein capture into ClyA-AS). We calculate the weighted average over time as the error in the bound fraction is non-linear, *e.g.* the error is lower near the K_d . The derivative of the ligand concentration is proportional to the determinate error (**equations 10 and 11, Supplementary Figure 6**), thus we calculated the weighted average based on this error estimation (**equations 12**), as well as the variance (**equation 13**).

$$[L](\theta) = \left(\frac{(\theta-a)*K_d}{a+b-\theta} \right)^{\frac{1}{n}} \quad (10)$$

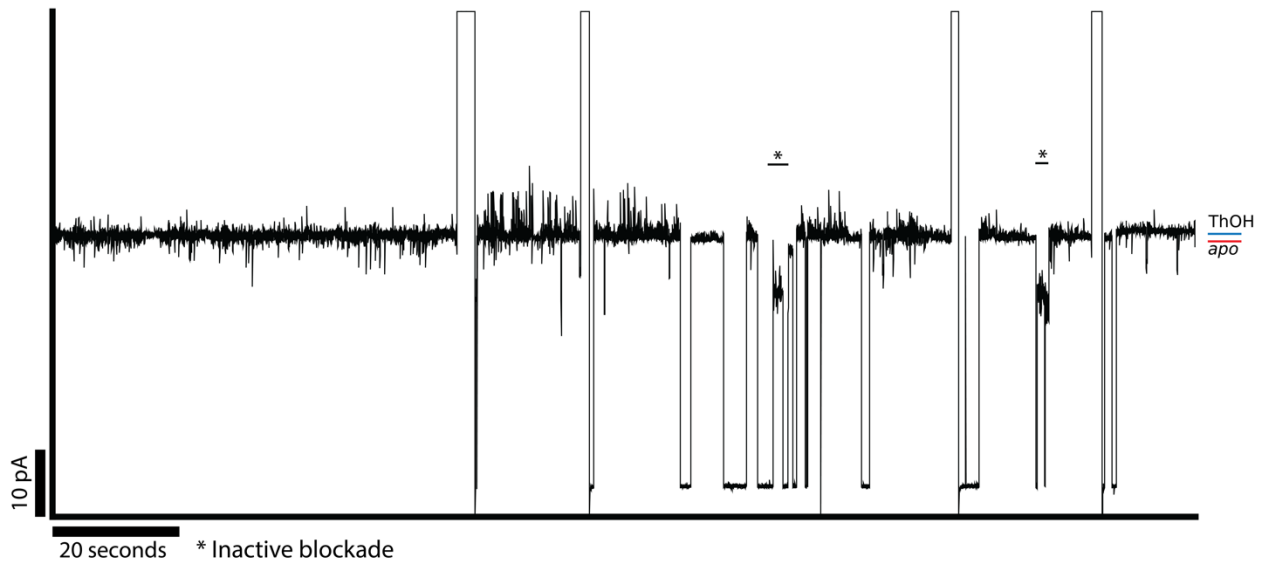
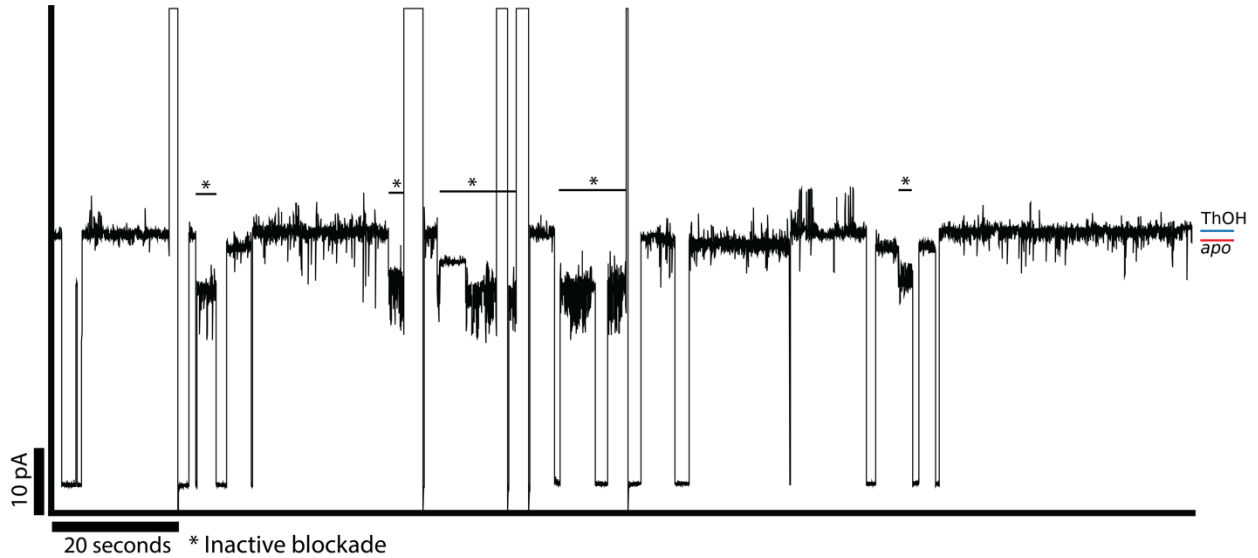
$$\frac{d}{d\theta} [L](\theta) = - \frac{b * \left(\frac{(\theta-a)*K_d}{a+b-\theta} \right)^{\frac{1}{n}}}{n(a-\theta)(a+b-\theta)} \quad (11)$$

$$\bar{\theta} = \frac{\sum_{i=1}^n \theta_i * \frac{d}{d\theta} [L](\theta_i)}{\sum_{i=1}^n \frac{d}{d\theta} [L](\theta_i)} \quad (12)$$

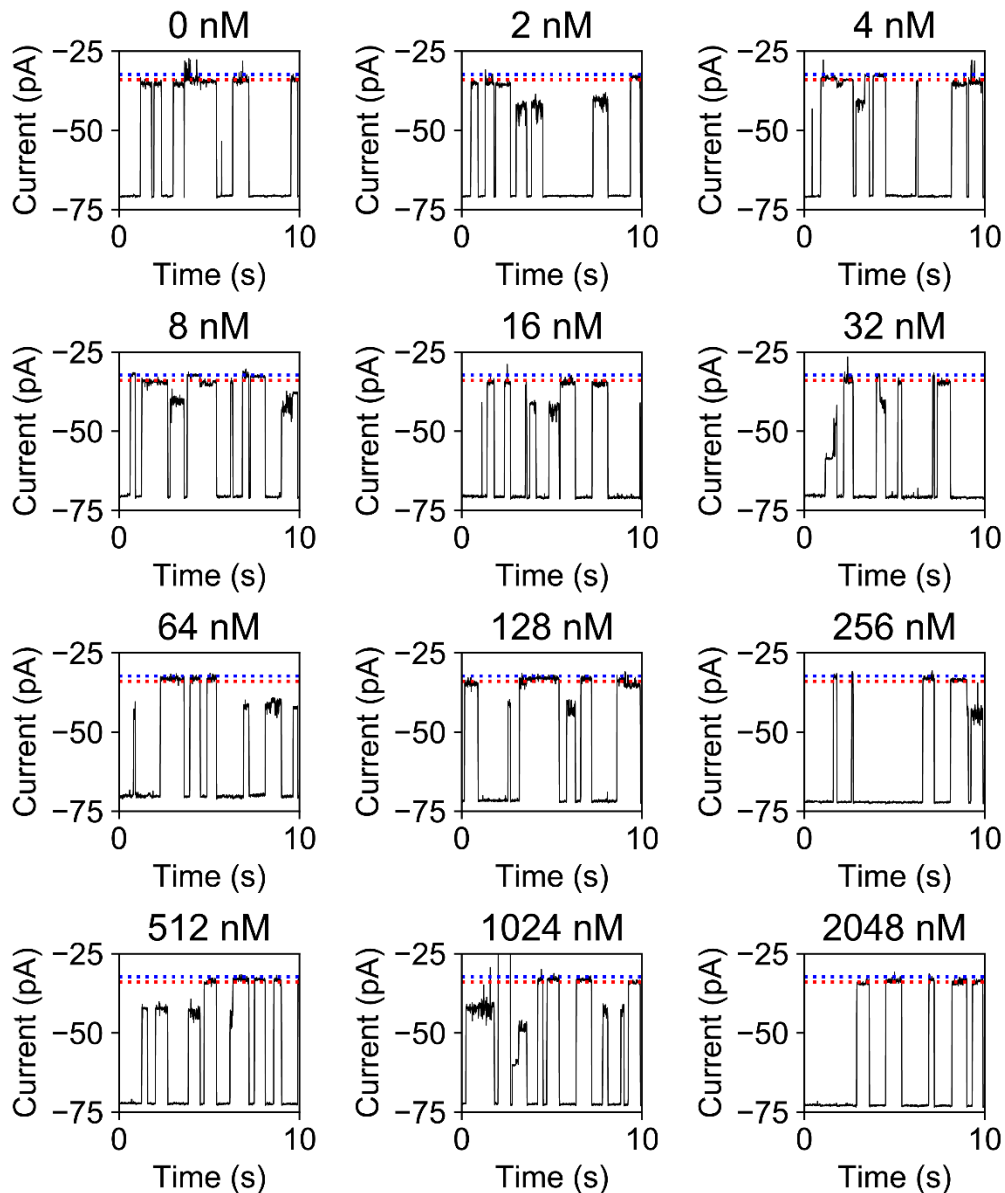
$$\sigma_{\theta}^2 = \frac{\sum_{i=1}^n \frac{d}{d\theta} [L](\theta_i) * (\theta_i - \bar{\theta})^2}{\sum_{i=1}^n \frac{d}{d\theta} [L](\theta_i)} \quad (13)$$



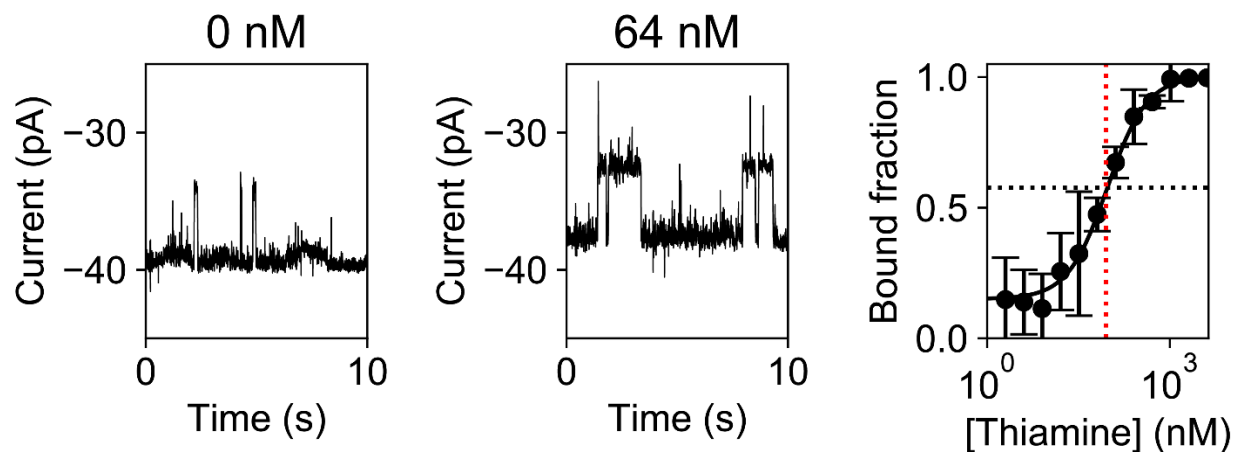
Inverse slope of the ligand concentration calculated from the bound fraction based on the Y27A-TbpA (added to *cis*) calibration. The bound fraction plotted against the slope of the ligand concentration for Y27A-TbpA (added to *cis*) calibration. The slope of the ligand concentration is calculated using equation 11.



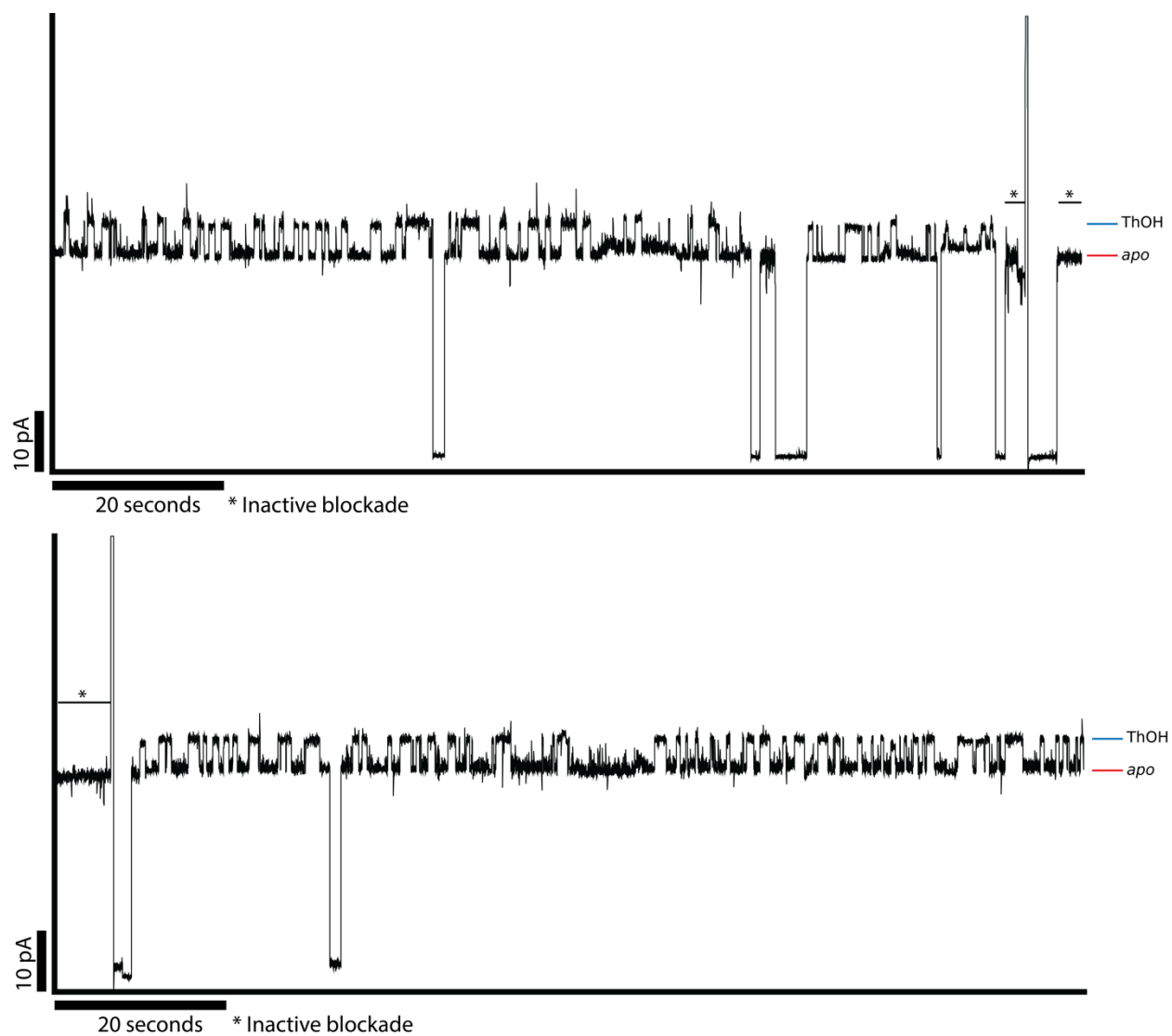
Supplementary Figure 1. Continuous trace of WT-TbpA in presence of thiamine Two parts of a continuous trace showing ionic current blockades elicited by WT-TbpA (15 nM, *cis*) to the C1yA nanopore displaying open and blocked pore currents. Thiamine-bound level (ThOH) and unbound (apo) level are denoted. Inactive blockades are marked with an asterisk. All measurements were performed on an Axon 200B amplifier with a 1550B digitizer in 150 mM NaCl supplemented with 15 mM Tris.HCl buffer (pH 7.5), at -45 mV at a sampling frequency of 10 kHz filtered to 2 kHz using a Bessel filter, all traces were digitally filtered to 100 Hz using a Gaussian filter. 64 nM thiamine is present (near the apparent K_D).



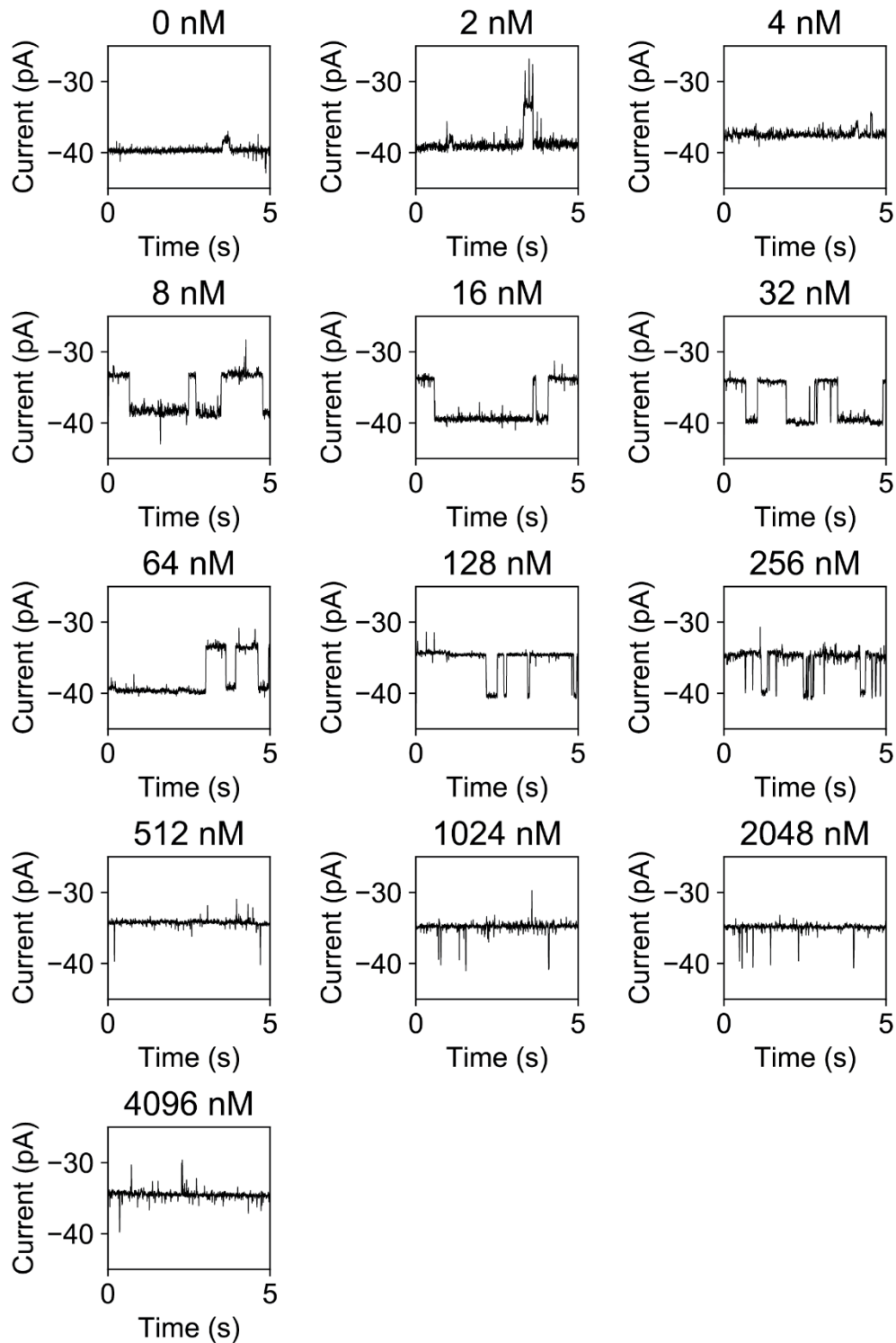
Supplementary Figure 2. Representative signal snippets of WT-TbpA with thiamine added to the *cis* chamber. Representative traces for WT thiamine binding protein (WT-TbpA, 15 nM, *cis*) using a protocol expelling the protein every few seconds, in the presence of thiamine, where thiamine was added to the *cis* compartment. The red dotted line represents the apo current and the blue dotted line represents the ligand bound current. All measurements were performed on an Axon 200B amplifier with a 1550B digitizer in 150 mM NaCl supplemented with 15 mM Tris.HCl buffer (pH 7.5), using a negative applied bias potential of 45 mV at a sampling frequency of 10 kHz filtered to 2 kHz using a Bessel filter, all traces were digitally filtered to 100 Hz using a Gaussian filter.



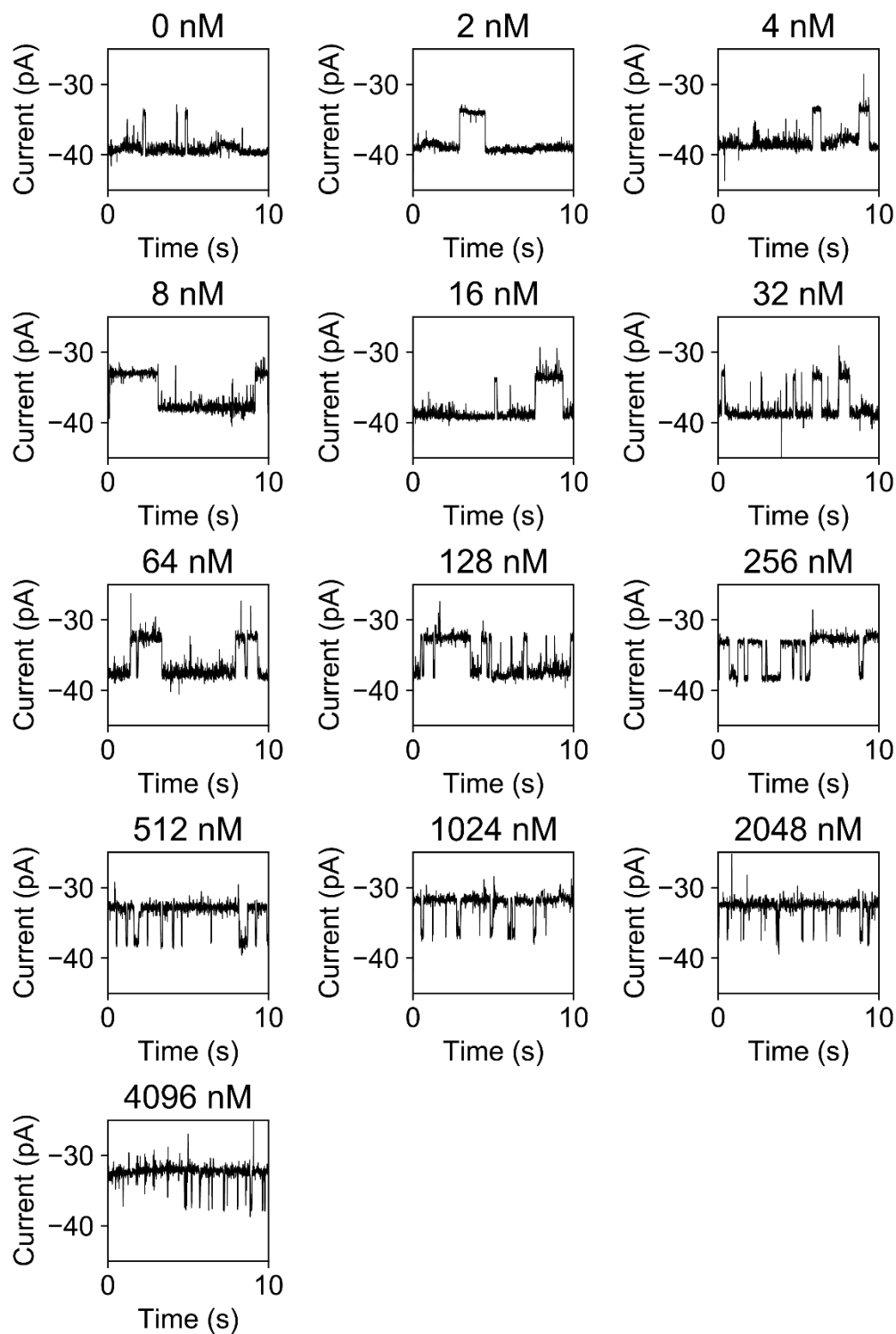
Supplementary Figure 3. Representative signal snippets and binding curves of Y27A-TbpA with thiamine added to *trans*. Representative traces for Y27A thiamine binding protein (Y27A-TbpA, 15 nM, *cis*), in the presence of thiamine, where thiamine was added to the *trans* compartment. The panel on the right shows the observed bound fraction set against the thiamine concentration, for Y27A-TbpA, addition of thiamine to the *trans* compartment. The dotted red line represents the K_d^{app} concentration. All measurements were performed on an Axon 200B amplifier with a 1550B digitizer in 150 mM NaCl supplemented with 15 mM Tris.HCl buffer (pH 7.5), using a negative applied bias potential of 45 mV at a sampling frequency of 10 kHz filtered to 2 kHz using a Bessel filter, all traces were digitally filtered to 100 Hz using a Gaussian filter.



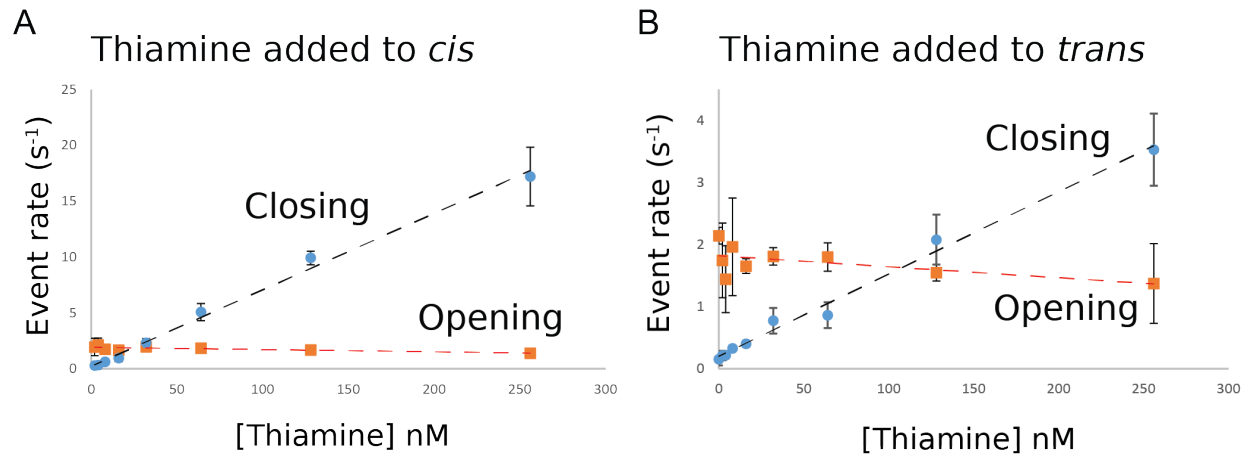
Supplementary Figure 4. Continuous trace of Y27A-TbpA in presence of thiamine Two parts of a continuous trace showing ionic current blockades elicited by Y27A-TbpA (15 nM, *cis*) to the ClyA nanopore. Thiamine-bound level (ThOH) and unbound (apo) level are denoted. Inactive blockades are marked with an asterisk. All measurements were performed on an Axon 200B amplifier with a 1550B digitizer in 150 mM NaCl supplemented with 15 mM Tris.HCl buffer (pH 7.5), at -45 mV at a sampling frequency of 10 kHz filtered to 2 kHz using a Bessel filter, all traces were digitally filtered to 100 Hz using a Gaussian filter. 16 nM thiamine is present (near the apparent K_D).



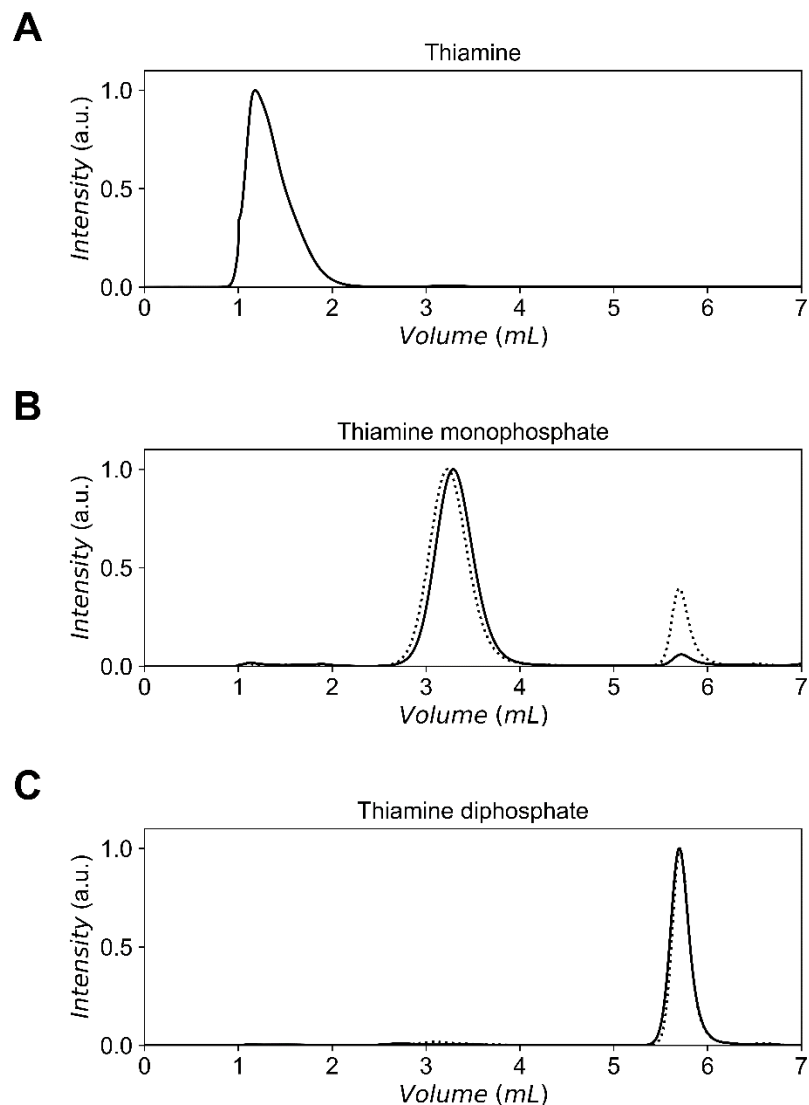
Supplementary Figure 5. Representative signal snippets of Y27A-TbpA with thiamine added to the *cis* chamber. Representative traces for Y27A thiamine binding protein (Y27A-TbpA, 15 nM, *cis*), in the presence of thiamine, where thiamine was added to the *cis* compartment. All measurements were performed on an Axon 200B amplifier with a 1550B digitizer in 150 mM NaCl supplemented with 15 mM Tris.HCl buffer (pH 7.5), using a negative applied bias potential of 45 mV at a sampling frequency of 10 kHz filtered to 2 kHz using a Bessel filter, all traces were digitally filtered to 100 Hz using a Gaussian filter.



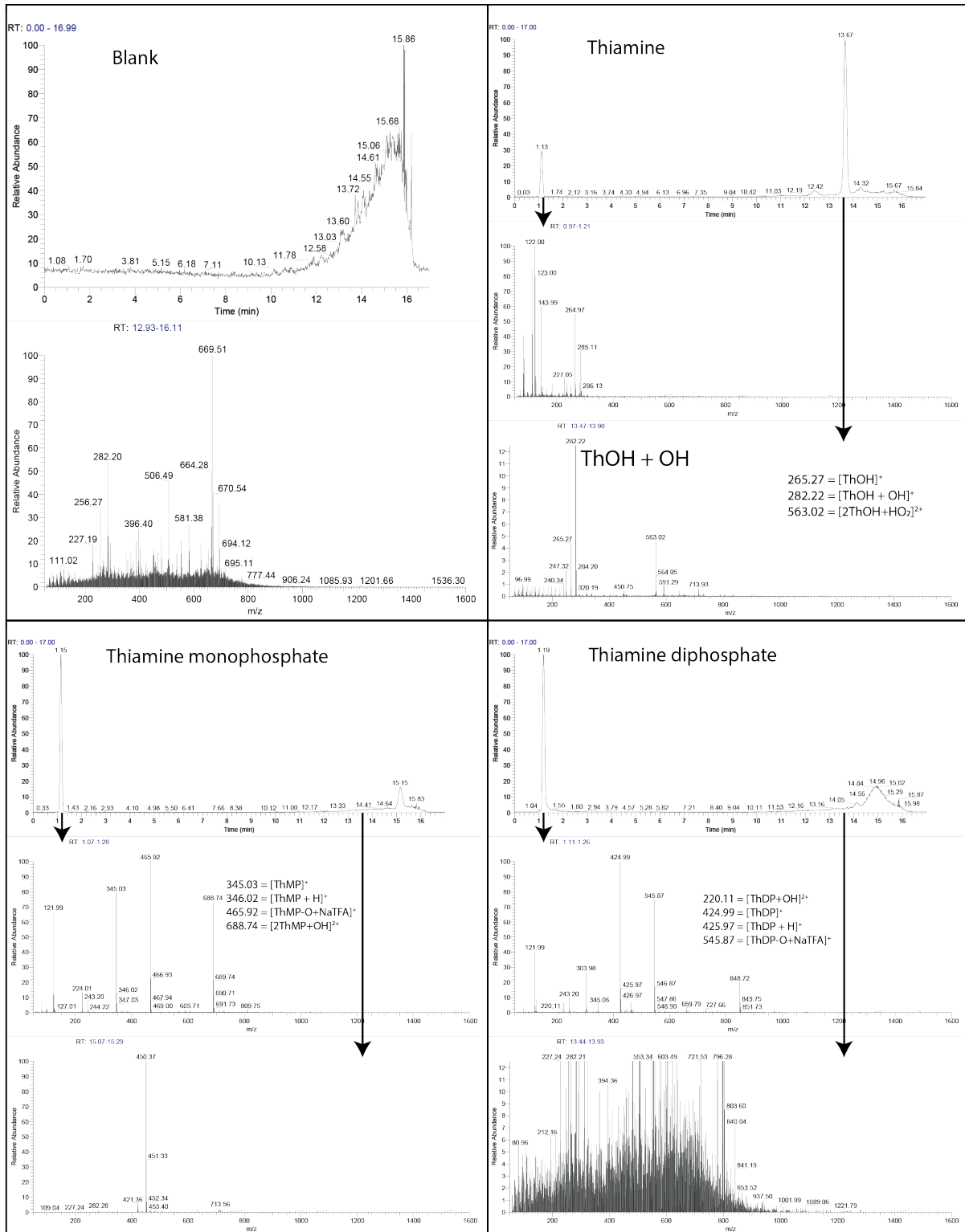
Supplementary Figure 6. Representative signal snippets of Y27A-TbpA with thiamine added to the *trans* chamber. Representative traces for Y27A thiamine binding protein (Y27A-TbpA, 15 nM, *cis*), in the presence of thiamine, where thiamine was added to the *trans* compartment. All measurements were performed on an Axon 200B amplifier with a 1550B digitizer in 150 mM NaCl supplemented with 15 mM Tris.HCl buffer (pH 7.5), using a negative applied bias potential of 45 mV at a sampling frequency of 10 kHz filtered to 2 kHz using a Bessel filter, all traces were digitally filtered to 100 Hz using a Gaussian filter.



Supplementary Figure 7. Apparent on- and off-rates of thiamine binding to Y27A-Thiamine binding protein. Opening and closing rates of thiamine binding Y27A-Thiamine binding protein (Y27A-TbpA, 15 nM, *cis*) relative to the concentration of thiamine added to (A) *cis* or (B) *trans*. The solid lines represent the best linear fit (1st order polynomial) through the concentration depend event rate. The rising (black) line represents the closing rate of Y27A-TbpA as the inverse event time of observed $I_{res}\%(apo)$. The decreasing (red) line represents the opening rate of Y27A-TbpA as the inverse event time of observed $I_{res}\%(thiamine)$. All measurements were performed on an Axon 200B amplifier with a 1550B digitizer in 150 mM NaCl supplemented with 15 mM Tris.HCl buffer (pH 7.5), using a negative applied bias potential of 45 mV at a sampling frequency of 10 kHz filtered to 2 kHz using a Bessel filter.



Supplementary Figure 8. FPLC result of thiamine and its phosphorylated derivatives. (A) thiamine, **(B)** thiamine monophosphate injected directly (solid line) and after incubation overnight at 37°C (dotted), **(C)** thiamine diphosphate injected directly (solid line) and after incubation overnight at 37°C (dotted). Experiments were performed using a HiTrap Q anion exchange column and a linear gradient between 0 M and 1 M NaCl buffered with 15 mM Tris to pH 7.5.



Supplementary Figure 9. LC/ESI-MS result of thiamine and its phosphorylated derivatives. The top-left figure shows the background control. The top-right figure shows thiamine elution at 13.7 minutes. The bottom-left figures show the thiamine monophosphate sample eluting at 1.1 minutes without thiamine diphosphate contamination and no thiamine near 13 minutes. The bottom-right figure shows the thiamine diphosphate eluting at 1.1 minutes without thiamine monophosphate contamination and no thiamine near 13 minutes.